Published online 27 November 2006 *Nucleic Acids Research, 2006, Vol. 34, No. 22* ***6521–6529***
doi:10.1093/nar/gkl892

Sequence-dependent formation of intrastrand crosslink products from the UVB irradiation of duplex DNA containing a 5-bromo-2′-deoxyuridine or 5-bromo-2′-deoxycytidine

Yu Zeng and Yinsheng Wang*

Department of Chemistry-027, University of California, Riverside, CA 92521-0403, USA

Received July 19, 2006; Revised October 4, 2006; Accepted October 9, 2006

ABSTRACT

The replacement of thymidine with 5-bromo-2′-deoxyuridine (^{Br}dU) is well-known to sensitize cells to ionizing radiation and photoirradiation. We reported here the sequence-dependent formation of intrastrand crosslink products from the UVB irradiation of duplex oligodeoxynucleotides harboring a ^{Br}dU or its closely related 5-bromo-2′-deoxycytidine (^{Br}dC). Our results showed that two types of crosslink products could be induced from d(^{Br}CG), d(^{Br}UG), d(G^{Br}U), or d(A^{Br}U); the C(5) of cytosine or uracil could be covalently bonded to the N(2) or C(8) of its neighboring guanine, and the C(5) of uracil could couple with the C(2) or C(8) of its neighboring adenine. By using those crosslink product-bearing dinucleoside monophosphates as standards, we demonstrated, by using liquid chromatography-mass spectrometry/mass spectrometry (LC-MS/MS), that all the crosslink products described above except d(G[N(2)-5]U) and d(G[N(2)-5]C) could form in duplex DNA. In addition, LC-MS/MS quantification results revealed that both the nature of the halogenated pyrimidine base and its 5′ flanking nucleoside affected markedly the generation of intrastrand crosslink products. The yields of crosslink products were much higher while the 5′ neighboring nucleoside was a dG than while it was a dA, and ^{Br}dC induced the formation of crosslink products much more efficiently than ^{Br}dU. The formation of intrastrand crosslink products from these halopyrimidines in duplex DNA may account for the photosensitizing effects of these nucleosides.

INTRODUCTION

The halogenated pyrimidine nucleoside, 5-bromo-2′-deoxyuridine (^{Br}dU), has been known for more than 40 years to be capable of sensitizing cells to both ionizing radiation (1–4) and photoirradiation (5–8). In this respect, partial replacement of thymidine with the isosteric ^{Br}dU in DNA increases considerably the amount of strand breaks and alkali labile sites in DNA induced from exposure to UV light and γ rays (6,9–12). Mechanistic studies suggested that the UV irradiation- or ionizing radiation-induced formation of the uracil-5-yl radical and subsequent hydrogen abstraction from the neighboring 5′ 2-deoxyribose by this radical are important for the formation of strand breaks (9,12,13). In addition, it was reported recently that the combination of another halogenated pyrimidine nucleoside, 5-bromo-2′-deoxycytidine (^{Br}dC), with the infection of an adenovirus expressing the Herpes simplex virus (HSV) thymidine kinase gene could result in significant radiosensitization of rat RT2 glioma cells (14). These studies revealed the potential clinical applications of ^{Br}dU and ^{Br}dC.

Recently we examined the photochemistry of duplex DNA harboring a ^{Br}dC and reported the facile formation of a type of intrastrand crosslink product where the C(5) of cytosine and the C(8) of its neighboring 5′ guanine are covalently bonded (15). We also demonstrated that the same crosslink product could form from unmodified DNA upon exposure to γ radiation (16). Similar UVB irradiation of duplex DNA harboring an A^{Br}CA sequence motif could lead to the formation of several types of intrastrand crosslink products (17).

Recent biochemical studies showed that intrastrand crosslink lesions may have important biological implications (16,18–20). In this regard, *in vitro* replication studies revealed that the crosslink lesion, where the C(5) of cytosine and the C(8) of its neighboring 5′ guanine are covalently bonded, could block DNA synthesis by replicative DNA polymerases (e.g. HIV reverse transcriptase and exonuclease-deficeint T7 DNA polymerase) (18) and lead to error-prone replication by the translesion synthesis DNA polymerase, yeast pol η (16). Furthermore, recent studies demonstrated that this and other structurely related intrastrand crosslink lesions could be subjected to repair by nucleotide excision repair with *Escherichia coli* UvrABC nuclease (19,20).

*To whom correspondence should be addressed. Tel: +1 951 827 2700; Fax: +1 951 827 4713; Email: yinsheng.wang@ucr.edu

© 2006 The Author(s).
This is an Open Access article distributed under the terms of the Creative Commons Attribution Non-Commercial License (http://creativecommons.org/licenses/by-nc/2.0/uk/) which permits unrestricted non-commercial use, distribution, and reproduction in any medium, provided the original work is properly cited.

To gain insights into the underlying mechanism for the photosensitizing effect of ^{Br}dU, it is important to examine whether intrastrand crosslink products can also be generated from the UV irradiation of ^{Br}dU-bearing DNA. In this context, recent studies showed that the exposure of duplex DNA carrying a ^{Br}dU in the bulge region to UV irradiation and γ radiation could lead to the formation of interstrand crosslink products (21–23). Moreover, there is a sequence selectivity (i.e. 5′-dA > 5′-dG) on the yields for strand cleavage from the UV irradiation of ^{Br}dU-bearing DNA (9). It remains unclear whether such a sequence selectivity also applies to the formation of intrastrand crosslink products from ^{Br}dU- or ^{Br}dC-bearing DNA.

Herein we explored the photo-crosslinking chemistry of ^{Br}dU- and ^{Br}dC-bearing duplex DNA, and we placed our emphasis on the structure elucidation of intrastrand crosslink products and the sequence-dependent formation of these products.

MATERIALS AND METHODS

Materials

All chemicals were obtained from Sigma-Aldrich (St. Louis, MO) unless otherwise specified. Calf intestinal alkaline phosphatase and nuclease P1 were from New England Biolabs (Beverly, MA) and US Biological (Swampscott, MA), respectively. The reagents used for solid-phase DNA synthesis were purchased from Glen Research Inc. (Sterling, VA).

Dinucleoside monophosphates d(G^{Br}U) and d(A^{Br}U) were synthesized following the previously reported procedures for the preparations of other dinucleoside monophosphates (Supplementary Schemes S1 and S2) (24,25). All other dinucleoside monophosphates and oligodeoxynucleotides (ODNs) containing a ^{Br}dU or ^{Br}dC were synthesized on a Beckman Oligo 1000S DNA synthesizer (Fullerton, CA) by using the commercially available phosphoramidite building blocks of ^{Br}dU and ^{Br}dC (Glen Research Inc.). The nucleobase deprotection was carried out in 29% ammonia at room temperature for 48 h, and the deprotection at room temperature was necessary for minimizing the decomposition of the halogenated nucleosides. The identities of all synthetic dinucleoside monophosphates and ^{Br}dU- or ^{Br}dC-containing ODNs were confirmed by ESI-MS and MS/MS analyses (Supplementary Figures S1 and S2).

UV irradiation

Dinucleoside monophosphate (100 nmol) was dissolved in 6 mL water and the solution was transferred to a 13 × 100 mm (O.D. × length) Pyrex tube (Catalog No. 99447-13, Corning Inc., Corning, NY). The 50% cut-off wavelength for the Pyrex tube was determined to be ~290 nm (17). Photoirradiation was carried out with a Hanovia 450-W medium-pressure mercury lamp, and the durations for photoirradiation were 90 min for d(^{Br}UG), 80 min for d(^{Br}CG), and 150 min for d(G^{Br}U) and d(A^{Br}U). During irradiation the Pyrex tube and lamp were immersed in an ice-water bath. During irradiation, the solution was exposed to, but not bubbled with, air. After irradiation, the mixture was dried by using a Savant Speed-vac (Savant Instrument Inc., Holbrook, New York). The dried residue was redissolved in water for high-performance liquid chromatography (HPLC) analysis.

For the irradiation of duplex ODNs, d(ATGGCG^{Br}UGCTAT), d(ATGGCG^{Br}CGCTAT), d(ATGGCA^{Br}CACTAT), or d(ATGGCA^{Br}UGCTAT) (50 nmol each), was annealed with its complementary strand in a buffer containing 50 mM NaCl and 50 mM phosphate (pH 6.8). The irradiation was carried out under aerobic conditions as described for the dinucleoside monophosphates except that the photoirradiations were continued for 10 or 90 min.

Enzymatic digestion

A 50 nmol photoirradiation mixture was dried by Speed-vac. Five units of nuclease P1, 0.005 U of calf spleen phosphodiesterase, 10 μL of 300 mM sodium acetate (pH 5.0), and water were added to make the final volume of the solution 250 μL. The digestion was carried out at 37°C for 6 h. The resulting solution was dried, and the dried residue was redissolved in a 250 μL solution containing 50 mM Tris–HCl (pH 8.6), 200 U of calf intestinal phosphatase, and 0.05 U of snake venom phosphodiesterase. The digestion was conducted at 37°C for 4 h. The digestion mixture was extracted with an equal volume of chloroform to remove the enzymes. The aqueous layer was dried and redissolved in water for liquid chromatography-mass spectrometry/mass spectrometry (LC-MS/MS) analysis.

HPLC

The HPLC separation was performed on a Surveyor system (ThermoFinnigan, San Jose, CA) with a photodiode array (PDA) detector, which was set at 260 nm for monitoring the effluents. Because of the low yields for crosslink products formed from d(G^{Br}U) and d(A^{Br}U), the PDA detector was set at 315 nm for the separation of irradiation mixtures of these two substrates. A 4.6 × 250 mm Apollo reverse-phase C18 column (5 μm in particle size and 300 Å in pore size, Alltech Associates Inc., Deerfield, IL) was used. A gradient of 5 min 0–3% acetonitrile followed by a 35 min 3–9% acetonitrile in 10 mM ammonium formate (pH 6.3) was employed, and the flow rate was 0.8 mL/min.

For NMR analysis, the products were further desalted by using a reversed-phase C18 column (10 × 250 mm, 5 μm in particle size, and 300 Å in pore size, Varian, Walnut Creek, CA). After the sample was loaded, the column was washed with water for 20 min, and the analyte was eluted from the column with an equal-volume solvent mixture of acetonitrile and water.

NMR measurement

All NMR spectra were recorded on a Varian Unity Inova 500 MHz instrument (Palo Alto, CA). The residual proton signal of the solvent served as internal reference. Two-dimensional (2-D) nuclear Overhauser effect spectroscopy (NOESY) experiments were performed at 298 K with 600 ms mixing time, and the NOE spectra were obtained from 2 × 256 × 2048 data matrices with 16–48 scans per t1 value.

Mass spectrometry

Electrospray ionization-mass spectrometry (ESI-MS) and tandem MS (MS/MS) experiments were conducted on an LCQ Deca XP ion-trap mass spectrometer (ThermoFinnigan, San Jose, CA). An equal-volume solvent mixture of acetonitrile and water was used as the carrier and electrospray solvent, and a 2 μL aliquot of 5 μM sample solution was injected in each run. The spray voltages were 4.5 and 3.0 kV for experiments in the positive- and negative-ion modes, respectively. The mass width for precursor ion selection in MS/MS and multi-stage MS modes was 3 *m*/*z* units. Each spectrum was obtained by averaging ~50 scans, and the time for each scan was 0.1 s.

LC-MS/MS

A Zorbax SB-C18 column (0.5 × 150 mm, Agilent Technologies, Palo Alto, CA) with a particle size of 5 μm was used for the separation of the above enzymatic digestion mixture. An Agilent 1100 capillary HPLC pump (Agilent Technologies) was employed for LC-MS/MS experiments. A 100 min gradient of 0–35% acetonitrile in 20 mM ammonium acetate was employed and the flow rate was 6.0 μL/min. The effluent was coupled to the LCQ Deca XP ion-trap mass spectrometer, which was operated in the positive-ion mode. The mass spectrometer was set up to alternate among MS, MS/MS, MS^3 and MS^4 modes. Purified crosslink product-bearing dinucleoside monophosphates were employed as external standards for the LC-MS/MS quantification experiments.

Determination of the extinction coefficients and the concentrations of standard intrastrand crosslink products

The extinction coefficients were determined by using a previously reported method (17). Because the two d(AˆU) products isolated from the irradiation mixture of d($A^{Br}U$) contained some contaminants, we did not determine the extinction coefficients of these products. Instead we quantified the concentrations of d(AˆU) in the stock solutions by using a similar NMR method. In this respect, we mixed d(AˆU) with a known amount of dT and quantified the amount of d(AˆU) in the mixture based on the ^{1}H-NMR spectrum of the mixture and the amount of dT added.

RESULTS

Formation of crosslink products from the Pyrex-filtered UV light irradiation of d(^{Br}UG) and d(G^{Br}U)

In the viewpoint that the Pyrex-filtered UV light irradiation of ^{Br}dC-containing duplex ODNs led to the covalent coupling of cytosine with its neighboring guanine or adenine (15,17), we decided to ask whether similar crosslinking chemistry occurs for ^{Br}dU-containing duplex ODNs. For the ease of characterization of crosslink products, we started with dinucleoside monophosphates d(^{Br}UG) and d(G^{Br}U), and indeed we were able to isolate two types of intrastrand crosslink products from the irradiation mixtures of either dinucleoside monophosphate.

Here we began our discussion with the products induced from d(^{Br}UG). Positive-ion ESI-MS of the fractions eluting at 14.1 and 32.3 min (Figure 1a) gave an ion of *m*/*z* 556, which was

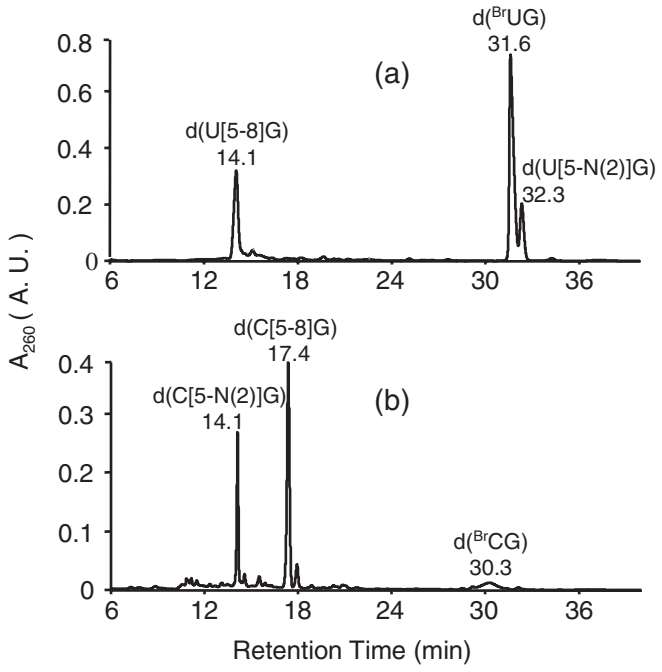

Figure 1. HPLC traces for the separation of the aerobic irradiation mixtures of d(^{Br}UG) (**a**) and d(^{Br}CG) (**b**).

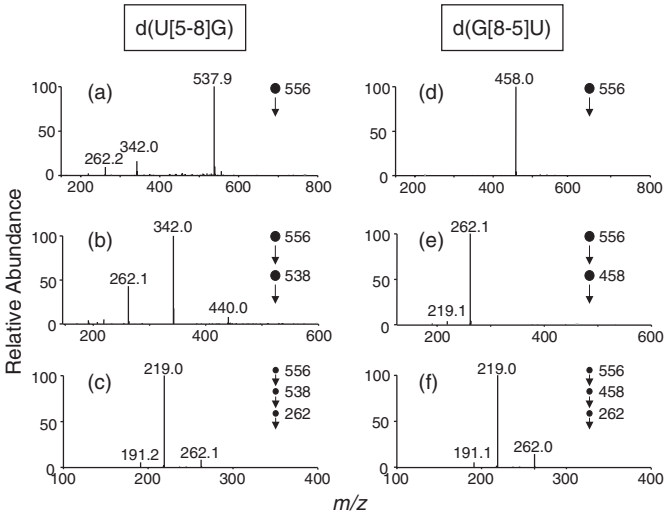

Figure 2. Positive-ion product-ion spectra of d(U[5-8]G): MS/MS (**a**), MS^3 (**b**), MS^4 (**c**) and d(G[8-5]U): MS/MS (**d**), MS^3 (**e**), MS^4 (**f**). The relative collisional energies were 30%.

2 a.m.u. less than the calculated *m*/*z* value of the $[M + H]^+$ ion of the unmodified d(UG). In addition, we failed to observe the bromine isotope pattern in the molecular ion peak. These results suggested that the products were initiated from the elimination of an HBr moiety from the starting d(^{Br}UG).

Product-ion spectra of the $[M + H]^+$ ions of the two products support that the two nucleobases in each product are covalently bonded. Collisional activation of the *m*/*z*-556 ion gives rise to a common and abundant fragment ion of *m*/*z* 538, which is attributed to the loss of a H_2O molecule (Figure 2a and Supplementary Figure S4a). Further breaking

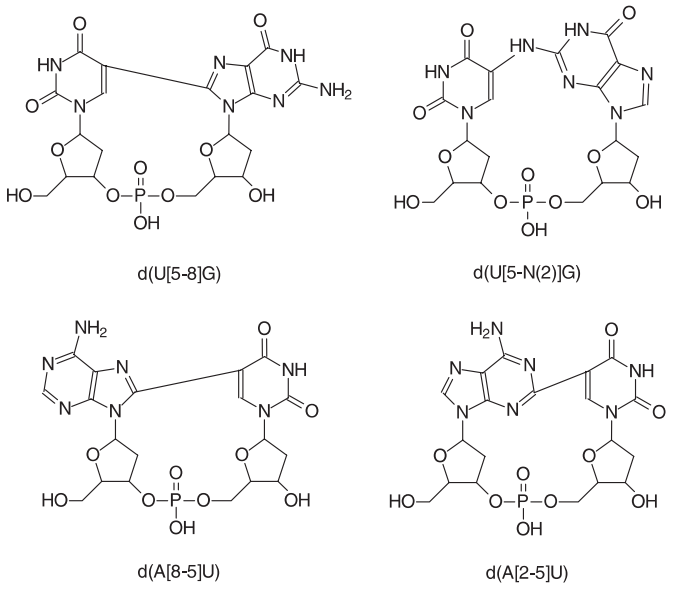

Scheme 1. Intrastrand crosslink products formed from d(^{Br}UG) and d(A^{Br}U).

down of the *m*/*z*-538 ion (MS/MS/MS, or MS^3) led to the formation of three common fragment ions of *m*/*z* 262, 342 and 440, though those ions are of different relative abundances for the two products (Figure 2b and Supplementary Figure S4b). The ions of *m*/*z* 440 and 342 are attributed to the neutral losses of a $C_5H_6O_2$ moiety (the 2-deoxyribose component) and the eliminations of both the $C_5H_6O_2$ moiety and an H_3PO_4 component, respectively. The presence of the ion of *m*/*z* 262, which is consistent with the calculated total masses of uracil and guanine with the elimination of two hydrogen atoms, reveals that uracil and guanine are covalently bound. Similar cleavages were observed for the fragmentation of other intrastrand crosslink lesions (15,17,24,25).

To further elucidate the structures of the two crosslink products, we recorded their ^{1}H-NMR and 2-D NOE spectra. ^{1}H-NMR spectrum of the 14.1 min fraction showed the presence of a singlet aromatic proton (Supplementary Figure S7a). The 2-D NOE spectrum of this product further allows us to assign all proton resonances (Supplementary Table S1). In addition, the 2-D NOESY showed that the aromatic proton resonance (δ 8.15 p.p.m.) exhibits strong correlations with the $H_{1'}$, $H_{2'}$, and $H_{3'}$ of the 5′ nucleoside as well as the $H_{1'}$ of the 3′ nucleoside, supporting that the aromatic proton is the H6 of uracil (A portion of the 2-D NOE spectrum is shown in Supplementary Figure S9a). The absence of the H(5) of uracil and the H(8) of guanine supports that the C(5) of uracil and the C(8) of guanine are covalently bonded. We, therefore, designate the product as d(U[5-8]G) (Structure shown in Scheme 1).

Next we examined the structure of the 32.3 min fraction by similar NMR analyses. Of the two aromatic proton resonances observed (Supplementary Figure S7b), one (δ 8.13 p.p.m.) exhibits a strong correlation peak with the $H_{1'}$ of the 3′ nucleoside and the other (δ 8.29 p.p.m.) correlates strongly with the $H_{1'}$ resonances of both the 5′ and 3′ nucleosides (Supplementary Figure S9b). These results facilitate the assignment of the two aromatic protons as the H(8) of guanine and the H(6) of uracil. The crosslink product, therefore, must bear a covalent bond between the C(5) of uracil and a heteroatom in guanine. Based on our detailed NMR characterizations of the corresponding crosslink product formed between cytosine and guanine (*vide infra*), we infer that the C(5) of uracil is covalently bonded with the N(2) of guanine and we designate the product as d(U[5-N(2)]G) (Scheme 2). In this context, it is worth noting that the covalent coupling to exocyclic NH_2 group was observed previously for crosslink products formed at neighboring adenine/cytosine (17) and cytosine/cytosine sites (24,26).

The two crosslink products also gave characteristic UV absorption spectra (Supplementary Figure S10a and b). Both crosslinks exhibited maximum absorbance at 260 nm, though they have distinctive absorption pattern in the wavelength range of 260–350 nm.

We next asked whether similar photo-crosslinking chemistry occurs for d(G^{Br}U). It turned out that the similar irradiation of d(G^{Br}U) yielded two analogous crosslink products, d(G[8-5]U) and d(G[N(2)-5]U) (See discussion on page S3 of the Supplementary Data).

Formation of crosslink products from the UVB irradiation of d(ATGGCG^{Br}UGCTAT)/ d(ATAGCACGCCAT)

After having characterized the structures of the crosslink products induced from d(^{Br}UG) and d(G^{Br}U), we next examined whether similar chemistry occurs in duplex ODN. To this end, we irradiated duplex **1** (Table 1) with UVB light, digested the irradiation mixture with four enzymes (i.e. nuclease P1, calf spleen phosphodiesterase, alkaline phosphatase and snake venom phosphodiesterase, see Experimental section), and analyzed the digestion mixture by LC-MS/MS. We chose these four enzymes because they have been employed successfully for the release of other intrastrand crosslink lesions from duplex ODNs (17,27,28).

To identify both d(G^U) and d(U^G) products, we set up an LC-MS/MS experiment to monitor the formation of the

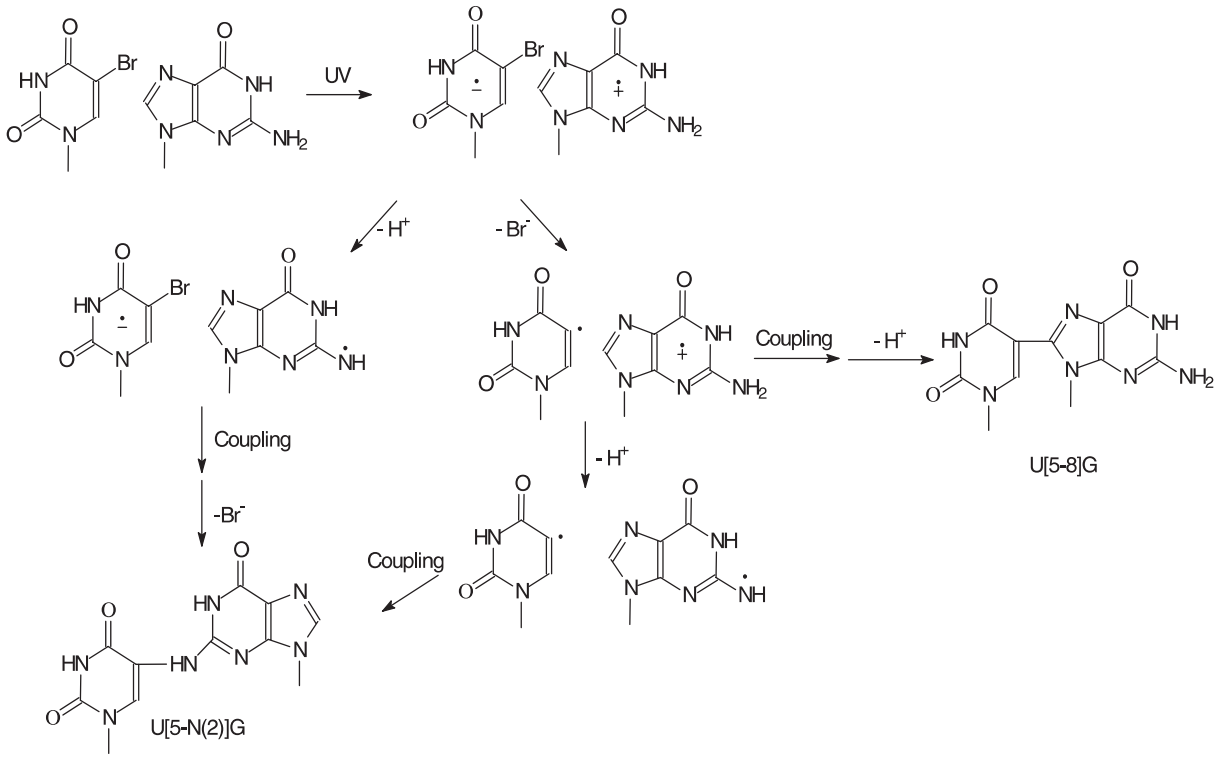

Scheme 2. Proposed mechanisms for the formation of intrastrand crosslink products between uracil and guanine.

Table 1. The ODN sequences employed for the Pyrex-filtered UV irradiation

Sequence number	Sequences
1	5′-d(ATGGCG^{Br}UGCTAT)-3′ 3′-d(TACCGC ACGATA)-5′
2	5′-d(ATGGCG^{Br}CGCTAT)-3′ 3′-d(TACCGC GCGATA)-5′
3	5′-d(ATGGCA^{Br}UGCTAT)-3′ 3′-d(TACCGT ACGATA)-5′
4	5′-d(ATGGCA^{Br}CACTAT)-3′ 3′-d(TACCGT GTGATA)-5′

fragment ions of *m*/*z* 458 and 538 from the precursor ion (*m*/*z* 556). It turned out that there is a major peak (18.0 min) in the selected-ion chromatogram (SIC) for the *m*/*z* 556→458 transition (Figure 3d). The 18.0 min fraction exhibits similar retention time and nearly identical MS^3/MS^4 as standard d(G[8-5]U) (Figure 3c versus 3d; Figure 2e and f versus Supplementary Figure S12a and d), supporting that this fraction bears d(G[8-5]U). In contrast, d(G[N(2)-5]U) was not detectable.

Similar analysis allowed us to conclude that the 18.6 and 30.4 min fractions contained d(U[5-8]G) and d(U[5-N(2)]G), respectively (Figure 3a versus 3b; Figure 2b and c versus Supplementary Figure S12b and e; Supplementary Figures S4b and c versus S12c and f). The 28.2 min fraction is an unknown product, which was not found in the irradiation mixture of d(^{Br}UG), and, due to the difficulty in obtaining it in large enough quantity from the enzymatic digestion products of the irradiation mixture, its structure was not examined. Thus, we identified three crosslink products from the UV irradiation of duplex **1**: U[5-8]G, U[5-N(2)]G, and G[8-5]U.

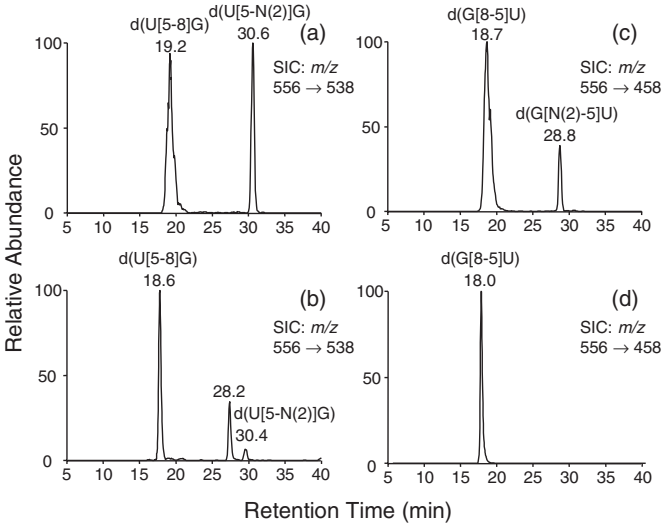

Figure 3. LC-MS/MS analysis of the standard d(U^G) (**a**) and d(G^U) (**c**) crosslink products and the enzymatic digestion products of the aerobic UVB-irradiated duplex ODN d(ATGGCG^{Br}UGCTAT)/d(ATAGCACGCCAT) (**b** and **d**). Shown are the SICs for the monitoring of the *m*/*z* 556→538 (a and b) and *m*/*z* 556→458 (c and d) transitions.

Formation of crosslink products from UVB irradiation of d(^{Br}CG)

We reported previously the isolation and characterization of d(C[5-8]G) as a major product formed from the Pyrex-filtered UV light irradiation of d(^{Br}CG) (15). The formation of both d(U[5-8]G) and d(U[5-N(2)]G) from the similar irradiation of d(^{Br}UG) prompted us to ask whether the irradiation of

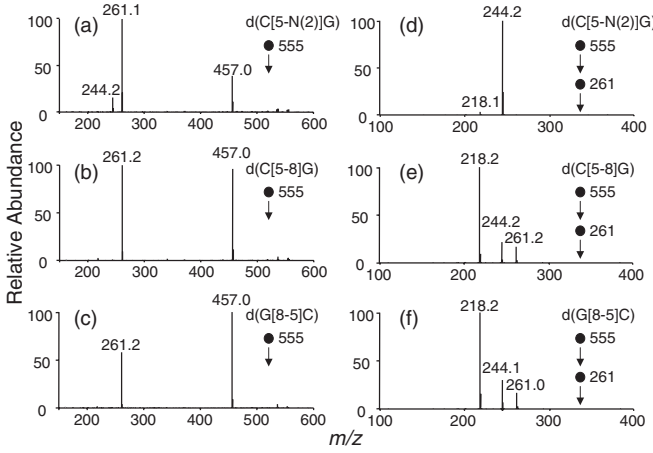

Figure 4. Positive-ion product-ion spectra of d(C[5-N(2)]G): MS/MS (**a**), MS^3 (**d**); d(C[5-8]G): MS/MS (**b**), MS^3 (**e**); and d(G[8-5]C): MS/MS (**c**), MS^3(**f**). The relative collisional energies were 30%.

d(^{Br}CG) can also result in the formation of d(C[5-N(2)]G). Indeed our results showed that this product could be induced.

Positive-ion ESI-MS of the HPLC fraction eluting at 14.1 min (Figure 1b) gave an ion of *m*/*z* 555, which is the same as the *m*/*z* of the $[M - H]^-$ ion of d(C[5-8]G). Moreover, MS/MS of the ion of *m*/*z* 555 showed the formation of the ions of *m*/*z* 457, 261, and 244 (Figure 4a). The former two fragment ions are attributed to the losses of $C_5H_6O_2$ and the 2-deoxyribose-phosphate backbone, respectively, whereas the ion of *m*/*z* 244 may form from the further elimination of an NH_3 from the ion of *m*/*z* 261. Collisional activation of the protonated ion of the crosslinked nucleobase portion, i.e. the ion of *m*/*z* 261, gives a MS^3 (Figure 4d) that is distinct from the corresponding MS^3 for d(C[5-8]G) or d(G[8-5]C) (Figure 4e and f). This result demonstrates that the two nucleobases in the crosslink product eluting at 14.1 min fraction are covalently bonded in a different fashion from those of d(C[5-8]G) and d(G[8-5]C).

The ^{1}H-NMR and 2-D NOE spectra provide further information about the structure of d(C[5-N(2)]G). The ^{1}H-NMR spectrum of the product shows the presence of two aromatic proton resonances (δ 8.06 and 8.11 p.p.m.) (Supplementary Figure S7c). In addition, a strong correlation peak between one aromatic proton (δ 8.06 p.p.m.) and the $H_{1'}$ of the 5′ nucleoside was found in the 2-D NOE spectrum, supporting that this aromatic proton is the H(6) of cytosine. Following the same rationale, we can assign the other aromatic proton (δ 8.11 p.p.m.) as the H(8) of guanine (Supplementary Figure S9c). The presence of the H(8) of guanine and the absence of the H(5) of cytosine support that the C(5) of cytosine is covalently bonded to a heteroatom in guanine.

We further concluded that the N(2) of guanine is coupled with the C(5) of cytosine based on the ^{1}H-NMR spectrum of this product in DMSO-d_6. In this respect, while DMSO-d_6 was used as solvent, the N(1)H proton in guanine and OH protons are sometimes difficult to be observed because the exchange with the residual H_2O occurs so rapidly that the averaged signal is broadened into the baseline (29). However, the N(2)H_2 protons in DMSO-d_6 exhibit an intermediate exchange rate with the trace amount of H_2O and observed as a somewhat broadened signal (29). When the ^{1}H-NMR spectra of d(C[5-N(2)]G) and dG in DMSO-d_6 are compared, we found the disappearance of N(2)H_2 signal at δ 6.56 p.p.m. and the appearance of a new signal at δ 9.52 p.p.m. for the crosslink product (Supplementary Figure S8). If the C(5) of cytosine were covalently bonded to the O(6) or N(1) of guanine, we would expect to observe intact signal for N(2)H_2 and the disappearance of the N(1)H signal, which, however, were not found in the ^{1}H-NMR spectrum. On the other hand, the observed marked downfield displacement of the remaining N(2)H proton is consistent with the covalent coupling of N(2) to the C(5) of cytosine. Therefore, the ^{1}H-NMR spectrum of d(C[5-N(2)]G) in DMSO-d_6 furnished unambiguous evidence for the structure assignment of this product.

Crosslink products formed from the UV irradiation of d(ATGGCG^{Br}CGCTAT)/d(ATAGCGCGCCAT) and d(ATGGCA^{Br}UGCTAT)/d(ATAGCATGCCAT)

Stimulated by the observation of both U[5-N(2)]G and U[5-8]G in the irradiation mixture of duplex DNA, we next investigated whether either or both of the two C^G crosslinks can also arise from the UV irradiation of duplex DNA containing a 5′-G^{Br}CG-3′ sequence motif. To this end, we irradiated a dodecameric duplex **2** (Table 1), degraded the mixture by same enzymes as what we used for duplex **1**, and analyzed the digestion products by LC-MS/MS.

Three standard crosslink products, i.e. d(C[5-N(2)]G), d(C[5-8]G) and d(G[8-5]C), were employed for the LC-MS/MS analysis, and the retention times for the three compounds were 20.3, 23.1 and 25.4 min, respectively (The SIC for monitoring the *m*/*z* 555→261 transition is shown in Figure 5a). The corresponding SIC for the analysis of the digestion mixture revealed that d(G[8-5]C) is the major crosslink product (25.1 min fraction, Figure 5b). Likewise, by comparing the retention time, MS^2, and MS^3, we determined that the minor components eluting at 20.6 and 23.2 min are d(C[5-8]G) and d(C[5-N(2)]G), respectively (Figures 4 and 5b and Supplementary Figure S13).

Therefore, the above results showed that three crosslink products, namely, C[5-8]G, C[5-N(2)]G and G[8-5]C, could be induced in duplex **2** upon UV irradiation.

We further demonstrated that the UVB light irradiation of d(A^{Br}U) and duplex DNA harboring an A^{Br}UG sequence motif (Duplex **3**, Table 1) could lead to the formation of two types of intrastrand crosslinks where the C(5) of uracil is covalently bonded to the C(2) or C(8) of its neighboring 5′ adenine (Scheme 1 and pages S3–S4 of the Supplementary Data). In this context, it is worth noting that we attempted, but failed to find the crosslink product where the C5 of uracil is covalently bonded to the N(6) of its neighboring 5′ adenine, which is consistent with the failure in detecting the analogous crosslink product formed at AC site (17).

Quantification of crosslink products formed from UV irradiation of duplex DNA

After having identified these crosslink products from the UV irradiation of ^{Br}dC- and ^{Br}dU-bearing duplex DNA, we next quantified the yields for the formation of these products. In this respect, we first determined the extinction coefficients

at 260 and 315 nm for the crosslink products based on Beer's Law and ^{1}H-NMR (17). With these extinction coefficients (Table 2), we determined the concentrations of the standard crosslink products.

Next, we subjected a series of standard solutions to LC-MS/MS experiments followed by analyzing the enzymatic digestion mixture under the same experimental conditions. The calibration curves were linear in the measured concentration range (Supplementary Table S2 and Supplementary Figure S11). Similar as what we carried out for the structurely related crosslink products (17,28), we also monitored the presence of all potential crosslink-containing trinucleoside diphosphates and tetranucleoside triphosphates by LC-MS/MS. It turned out that the incomplete digestion products account for <5% of the dinucleoside monophosphate products (data not shown).

The quantification results allowed us to determine that the neighboring 5′ nucleoside being dA or dG and the halogenated nucleoside being ^{Br}dU or ^{Br}dC can both affect the yields of the crosslink products (Table 3). First, the nature of the 5′ flanking nucleoside affects significantly the yields of the crosslink products. Under aerobic conditions, irradiation of duplex DNA containing a 5′-G^{Br}X-3′ (^{Br}X = ^{Br}dC or ^{Br}dU) sequence motif gives much higher yields for crosslink products than duplex DNA harboring a 5′-A^{Br}X-3′ sequence component. In this regard, the yield of G[8-5]C from duplex **2** is ~17%, which is 7-fold higher than the combined yield of two AˆC crosslinks (2.4%) from duplex **4** (Table 3, all the yields in this and the following discussion refer to the 10 min irradiation mixtures). Because of the high yield, the G[8-5]C-bearing ODN could be readily isolated from the irradiation mixture of duplex **2** by HPLC (Supplementary Figure S16) (15). Similarly, the yield of G[8-5]U from duplex **1** is ~0.5%, which is 4 times as high as the total yield of the two AˆU products from duplex **3** (0.12%).

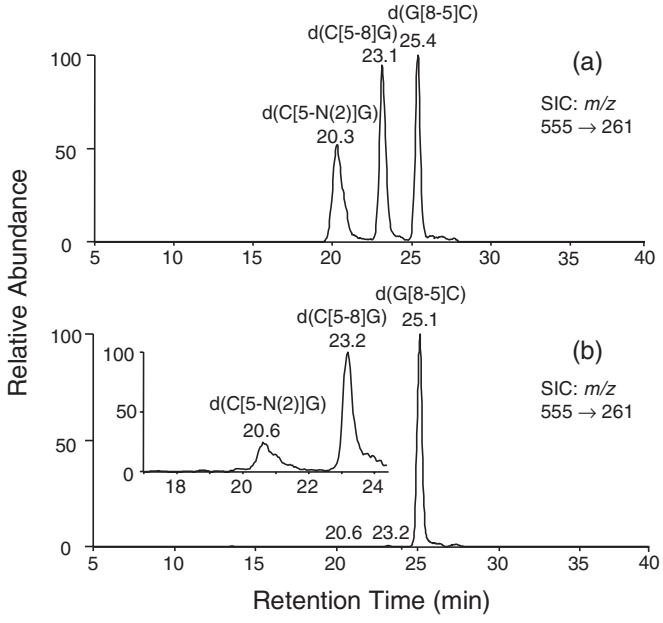

Figure 5. LC-MS/MS analysis of the standard d(CˆG) and d(GˆC) crosslink products (**a**) and the enzymatic digestion products of the UVB-irradiated duplex ODN d(ATGGCG^{Br}CGCTAT)/d(ATAGCGCGCCAT) (**b**). Shown are the SICs for monitoring the *m/z* 555→261 transition. A portion of SIC for the analysis of the digestion products was plotted in a different scale to better view the formation of the two CˆG crosslinks [inset in (b)].

Second, the two halogenated nucleosides exhibit marked difference in efficiency of inducing the crosslink products. The data in Table 3 showed that the total yield of three crosslink products from **2** (18%) was >20-fold higher than that from **1** (0.7%). Likewise, the combined yield of the two crosslink products from **4** (2.4%) was ~20 times greater than that from **3** (0.12%). Thus, ^{Br}dC is more efficient in inducing the formation of crosslink products than ^{Br}dU. Third, we found that the yields for GˆU and GˆC are higher than those for UˆG and CˆG, respectively (Table 3). Similar sequence-dependent formation of intrastrand crosslink products was observed for the 90 min irradiation mixtures (Table 3).

The above sequence-dependent formation of intrastrand crosslink products might be addressed from the relative stacking energies between the halogenated nucleobase and its neighboring purine base in different sequence contexts. In this respect, Ornstein *et al*. (30) calculated the total stacking energy for the possible dimers of neighboring B-form DNA pairs, in which the corrected optimized potential of 5′-GC-3′/5′-GC-3′, 5′-AC-3′/5′-GT-3′, and 5′-AT-3′/5′-AT-3′ are −14.59, −10.51 and −6.57 kcal/mol, respectively. If we assume that the stacking energies of 5′-G^{Br}C-3′/5′-GC-3′, 5′-A^{Br}C-3′/5′-GT-3′, 5′-G^{Br}U-3′/5′-AC-3′ and 5′-A^{Br}U-3′/5′-AT-3′ are similar as those of 5′-GC-3′/5′-GC-3′, 5′-AC-3′/5′-GT-3′, 5′-AC-3′/5′-GT-3′ and 5′-AT-3′/5′-AT-3′, respectively, the stacking preference follows the order of 5′-dG > 5′-dA for both ^{Br}dC- and ^{Br}dU-containing ODNs. In addition, the stacking is more favorable for ^{Br}dC than for ^{Br}dU regardless of the identity of the 5′ flanking nucleoside being a dG or dA. Moreover, 5′-Purine•Pyrimidine-3′ site always stacks better than the same composing nucleosides arranged in the order of 5′-Pyrimidine•Purine-3′ (30). This, combined with the quantification results, supports that the yield of crosslink product is higher while the stacking is more favorable. The favorable stacking of the halogenated nucleoside with its vicinal purine nucleoside is expected to promote the photo-induced electron transfer between the two neighboring nucleobases, which results in more efficient formation of the intrastrand crosslink products (*vide infra*). In this context, it is worth noting that guanine has lower ionization potential than adenine (31,32), which may also contribute, to some extent, to the more efficient electron transfer to the neighboring halogenated nucleoside while the adjacent 5′ nucleoside is a dG than while it is a dA.

Table 2. The extinction coefficients (ε_{260} and ε_{315}, units in L/mol/cm) for the crosslink products discussed in this paper

	U[5-8]G	U[5-N(2)]G	G[8-5]U	G[N(2)-5]U	C[5-N(2)]G	C[5-8]G	G[8-5]C
ε_{260}	18 800	28 000	19 000	23 300	24 500	20 300	22 800
ε_{315}	8700	9400	5900	10 400	2800	12 600	11 400

Table 3. The yields for the crosslink products generated from the UVB irradiation of ^{Br}dU and ^{Br}dC-containing duplex ODNs

Substrate	[5-N(2)]/[5-N(6)]	[5-8]	[5-2]	[8-5]	[2-5]
10 min irradiation					
5′-G^{Br}CG-3′ (**2**)	0.5 ± 0.2	0.22 ± 0.08	—	17 ± 8	—
5′-A^{Br}CA-3′ (**4**)	0.6 ± 0.4	0.5 ± 0.3	0.3 ± 0.1	1.6 ± 0.7	0.8 ± 0.4
5′-G^{Br}UG-3′ (**1**)	—	0.16 ± 0.05	—	0.5 ± 0.1	—
5′-A^{Br}UG-3′ (**3**)	—	—	—	0.09 ± 0.03	0.03 ± 0.01
90 min irradiation					
5′-G^{Br}CG-3′ (**2**)	0.23 ± 0.08	0.16 ± 0.05	—	40 ± 16	—
5′-A^{Br}CA-3′ (**4**)	0.3 ± 0.2	0.5 ± 0.2	0.26 ± 0.04	2 ± 1	0.6 ±0.4
5′-G^{Br}UG-3′ (**1**)	0.2 ± 0.2	1.1 ± 0.2	—	3 ± 1	—
5′-A^{Br}UG-3′ (**3**)	—	—	—	0.10 ± 0.05	0.05 ± 0.02

The yields refer to percent conversions of the parent duplex and the results represent the means and SDs from 3 to 6 independent measurements.

Proposed mechanisms for the formation of crosslink products induced from UV irradiation

Based on the previous investigation on the photoactivation of 5-halopyrimidines (9,15,17,33,34), we reason that the Pyrex-filtered UV irradiation can lead to the transferring of an electron from guanine to the neighboring 5-bromouracil or 5-bromocytosine. The resulting anion radical of the halogenated nucleobase can then eliminate a bromide ion to yield the 5-yl radical of uracil or cytosine. The pyrimidin-5-yl radicals can subsequently couple with the C(8) of the neighboring purine base, and the resulting products can deprotonate to offer crosslink products X[5-8]G and G[8-5]X (X = C or U).

The formation of X[5-N(2)]G or G[N(2)-5]X may follow a different mechanism. The cation radical of 2′-deoxyguanosine may deprotonate to give an N(2)-centered radical (35), which can couple with the 5-yl anion radical of the neighboring uracil or cytosine followed by losing the bromide ion to give the crosslink products. Alternatively, the N(2) cation radical of guanine might first couple with 5-yl radical of uracil or cytosine, then deprotonate to generate crosslink products (Scheme 2). The formation of the two A^U crosslink products may follow similar mechanisms as what we proposed for the formation of the two A^C crosslinks (Supplementary Scheme S3) (17).

With regard to the proposed mechanism, the formation of guanine radical cation may lead to the generation of 8-oxo-2′-deoxyguanosine (8-oxodG). LC-MS/MS analysis showed that 8-oxodG indeed could be induced from the UVB irradiation of all four halopyrimidine-bearing duplex ODNs; however, the yields for the formation of this product from 5-halopyrimidine-containing duplexes are not significantly higher than those from the control unmodified ODNs (data not shown). Along this line, we were unable to isolate, from the UVB irradiation mixture of duplex **2**, a pure ODN where the 2′-deoxyguanosine residue on the 5′ or 3′ side of ^{Br}dC has been converted to an 8-oxodG. These observations may suggest that the coupling of the radical cation with its neighboring pyrimidilyl radical occurs more readily than its decay to give 8-oxodG.

The radical anion of 5-bromocytosine, 5-bromouracil, or their corresponding pyrimidilyl radicals may conceivably couple with molecular oxygen and result in the formation of other products. However, HPLC analysis of the irradiation mixture of duplex **2** under saturated oxygen conditions showed that such irradiation could lead to the formation of G[8-5]C-bearing ODN in ~40% yield (Supplementary Figure S16). This result, therefore, demonstrates that coupling with the neighboring guanine is a favorable pathway even in the presence of excess amount of molecular oxygen.

DISCUSSION

We showed that the Pyrex-filtered UV light irradiation of d(^{Br}UG), d(^{Br}CG) and d(G^{Br}U) gave rise to two types of crosslink products where the C(5) of cytosine or uracil is covalently bonded to the C(8) or N(2) of its neighboring guanine. The similar irradiation of d(A^{Br}U) resulted in the formation of d(A[8-5]U) and d(A[2-5]U).

The crosslink products induced in dinucleoside monophosphates can also arise from 5-bromocytosine- or 5-bromouracil-harboring duplex ODNs upon UV irradiation. In this respect, three types of crosslink isomers, i.e. G[8-5]X, X[5-8]G and X[5-N(2)]G, are generated from ODNs harboring a 5′-G^{Br}XG-3′ sequence motif. On the other hand, UV irradiation of ODNs containing a 5′-A^{Br}U-3′ sequence component led to the formation of two isomeric crosslink products, A[8-5]U and A[2-5]U. Although it has been shown that the UV irradiation of bulged DNA sequences containing a ^{Br}dU can lead to the formation of interstrand crosslink (23), this is the first demonstration that the UV irradiation of ^{Br}dU-bearing, fully complementary duplex DNA can give rise to the formation of intrastrand crosslink products. Except for C[5-8]G and G[8-5]C, other crosslink products were reported here for the first time.

In contrast to what was observed for the formation of strand break products (9), there is a thermodynamic sequence selectivity (5′-dG > 5′-dA) for UVB-induced crosslink products in ODNs containing a ^{Br}dU or ^{Br}dC. In addition, ^{Br}dC is more efficient than ^{Br}dU in inducing crosslink products from the studied ODNs by UV irradiation. The above observations are consistent with the proposed electron transfer mechanism for the formation of the crosslink products and strongly suggest that stacking between the halogenated base and its neighboring purine base affects significantly the yields for the formation of crosslink products.

On the grounds that this type of intrastrand crosslink product can block DNA replication and introduce errors during translesion synthesis (16,18), the formation of intrastrand crosslink products may account, at least partly, for the

enhanced sensitivity of living cells to UV irradiation resulting from the substitution of thymidine with ^{Br}dU (5–8). The unambiguous identification of the intrastrand crosslink products formed from synthetic duplex DNA sets a stage for the detection of these lesions formed *in vivo* and for understanding the biological implications of these lesions.

SUPPLEMENTARY DATA

Supplementary Data are avialable at NAR Online.

ACKNOWLEDGEMENTS

The authors thank the National Institutes of Health for supporting this research (R01 CA96906). Funding to pay the Open Access publication charges for this article was provided by the National Institutes of Health.

REFERENCES

1. Dewey,W.C. and Humphrey,R.M. (1965) Increase in radiosensitivity to ionizing radiation related to replacement of thymidine in mammalian cells with 5-bromodeoxyuridine. *Radiat. Res.*, **26**, 538–553.
2. Sano,K., Hoshino,T. and Nagai,M. (1968) Radiosensitization of brain tumor cells with a thymidine analogue (bromouridine). *J. Neurosurg.*, **28**, 530–538.
3. Ling,L.L. and Ward,J.F. (1990) Radiosensitization of Chinese hamster V79 cells by bromodeoxyuridine substitution of thymidine: enhancement of radiation-induced toxicity and DNA strand break production by monofilar and bifilar substitution. *Radiat. Res.*, **121**, 76–83.
4. Webb,C.F., Jone,G.D., Moyer,D.J., Aguilera,J.A. and Ling,L.L. (1993) Mechanisms of radiosensitization in bromodeoxyuridine-substituted cells. *Int. J. Radiat. Biol.*, **64**, 695–705.
5. Taguchi,T. and Shiraishi,Y. (1989) Increased sister-chromatid exchanges (SCEs) and chromosomal fragilities by BrdU in a human mutant B-lymphoblastoid cell line. *Mutat. Res.*, **211**, 43–49.
6. Cadet,J. and Vigny,P. (1990) In Morrison,H. (ed.), *Bioorganic Photochemistry*. John Wiley, New York, Vol. 1, pp. 1.
7. Ribas,M., Korenberg,J.R., Peretti,D., Pichiri,G., Stockert,J.C., Gosalvez,J. and Mezzanotte,R. (1994) Sister chromatid differentiation in 5-bromo-2′-deoxyuridine-substituted chromosomes: a study with DNA-specific ligands and monoclonal antibody to histone H2B. *Chromosome Res.*, **2**, 428–438.
8. Wojcik,A., von Sonntag,C. and Obe,G. (2003) Application of the biotin-dUTP chromosome labelling technique to study the role of 5-bromo-2′-deoxyuridine in the formation of UV-induced sister chromatid exchanges in CHO cells. *J. Photochem. Photobiol. B: Biol.*, **69**, 139–144.
9. Sugiyama,H., Tsutsumi,Y. and Saito,I. (1990) Highly sequence-selective photoreaction of 5-bromouracil-containing deoxyhexanucleotides. *J. Am. Chem. Soc.*, **112**, 6720–6721.
10. Fuciarelli,A.F., Sisk,E.C. and Zimbrick,J.D. (1994) Electron migration in oligonucleotides upon gamma-irradiation in solution. *Int. J. Radiat. Biol.*, **65**, 409–418.
11. Limoli,C.L., Wu,C.C., Milligan,J.R. and Ward,J.F. (1997) Photochemical production of uracil quantified in bromodeoxyuridine-substituted SV40 DNA by uracil DNA glycosylase and a lysyl-tyrosyl-lysine tripeptide. *Mutagenesis*, **12**, 443–447.
12. Chen,T., Cook,G.P., Koppisch,A.T. and Greenberg,M.M. (2000) Investigation of the origin of the sequence selectivity for the 5-halo-2′-deoxyuridine sensitization of DNA to damage by UV-irradiation. *J. Am. Chem. Soc.*, **122**, 3861–3866.
13. Cook,G.P., Chen,T., Koppisch,A.T. and Greenberg,M.M. (1999) The effects of secondary structure and O_2 on the formation of direct strand breaks upon UV irradiation of 5-bromodeoxyuridine-containing oligonucleotides. *Chem. Biol.*, **6**, 451–459.
14. Brust,D., Feden,J., Farnsworth,J., Amir,C., Broaddus,W.C. and Valerie,K. (2000) Radiosensitization of rat glioma with bromodeoxycytidine and adenovirus expressing herpes simplex virus-thymidine kinase delivered by slow, rate-controlled positive pressure infusion. *Cancer Gene Ther.*, **7**, 778–788.
15. Zeng,Y. and Wang,Y. (2004) Facile formation of an intrastrand cross-link lesion between cytosine and guanine upon Pyrex-filtered UV light irradiation of d(^{Br}CG) and duplex DNA containing 5-bromocytosine. *J. Am. Chem. Soc.*, **126**, 6552–6553.
16. Gu,C. and Wang,Y. (2004) LC-MS/MS identification and yeast polymerase eta bypass of a novel gamma-irradiation-induced intrastrand cross-link lesion G[8-5]C. *Biochemistry*, **43**, 6745–6750.
17. Hong,H. and Wang,Y. (2005) Formation of intrastrand cross-link products between cytosine and adenine from UV irradiation of d(^{Br}CA) and duplex DNA containing a 5-bromocytosine. *J. Am. Chem. Soc.*, **127**, 13969–13977.
18. Gu,C. and Wang,Y. (2005) Thermodynamic and *in vitro* replication studies of an intrastrand crosslink lesion G[8-5]C. *Biochemistry*, **44**, 8883–8889.
19. Yang,Z., Colis,L.C., Basu,A.K. and Zou,Y. (2005) Recognition and incision of gamma-radiation-induced cross-linked guanine-thymine tandem lesion G[8,5-Me]T by UvrABC nuclease. *Chem. Res. Toxicol.*, **18**, 1339–1346.
20. Gu,C., Zhang,Q., Yang,Z., Wang,Y., Zou,Y. and Wang,Y. (2006) Recognition and incision of oxidative intrastrand cross-link lesions by UvrABC nuclease. *Biochemistry*, **45**, 10739–10746.
21. Cecchini,S., Girouard,S., Huels,M.A., Sanche,L. and Hunting,D.J. (2004) Single-strand-specific radiosensitization of DNA by bromodeoxyuridine. *Radiat. Res.*, **162**, 604–615.
22. Cecchini,S., Girouard,S., Huels,M.A., Sanche,L. and Hunting,D.J. (2005) Interstrand cross-links: a new type of gamma-ray damage in bromodeoxyuridine-substituted DNA. *Biochemistry*, **44**, 1932–1940.
23. Cecchini,S., Masson,C., La Madeleine,C., Huels,M.A., Sanche,L., Wagner,J.R. and Hunting,D.J. (2005) Interstrand cross-link induction by UV radiation in bromodeoxyuridine-substituted DNA: Dependence on DNA conformation. *Biochemistry*, **44**, 16957–16966.
24. Liu,Z., Gao,Y. and Wang,Y. (2003) Identification and characterization of a novel cross-link lesion in d(CpC) upon 365-nm irradiation in the presence of 2-methyl-1,4-naphthoquinone. *Nucleic Acids Res.*, **31**, 5413–5424.
25. Zhang,Q. and Wang,Y. (2003) Independent generation of 5-(2′-deoxycytidinyl)methyl radical and the formation of a novel crosslink lesion between 5-methylcytosine and guanine. *J. Am. Chem. Soc.*, **125**, 12795–12802.
26. Liu,Z., Gao,Y., Zeng,Y., Fang,F., Chi,D. and Wang,Y. (2004) Isolation and characterization of a novel cross-link lesion in d(CpC) induced by one-electron photooxidation. *Photochem. Photobiol.*, **80**, 209–215.
27. Bellon,S., Ravanat,J.L., Gasparutto,D. and Cadet,J. (2002) Cross-linked thymine-purine base tandem lesions: synthesis, characterization, and measurement in gamma-irradiated isolated DNA. *Chem. Res. Toxicol.*, **15**, 598–606.
28. Zhang,Q. and Wang,Y. (2005) Generation of 5-(2′-deoxycytidyl)methyl radical and the formation of intrastrand cross-link lesions in oligodeoxyribonucleotides. *Nucleic Acids Res.*, **33**, 1593–1603.
29. West,R.T., Garza,L.A., 2nd, Winchester,W.R. and Walmsley,J.A. (1994) Conformation, hydrogen bonding and aggregate formation of guanosine 5′-monophosphate and guanosine in dimethylsulfoxide. *Nucleic Acids Res.*, **22**, 5128–5134.
30. Ornstein,R.L. (1978) An optimized potential function for the calculation of nucleic acid interaction energies. I. Base stacking. *Biopolymers*, **17**, 2341–2360.
31. Seidel,C.A.M., Schulz,A. and Sauer,M.H.M. (1996) Nucleobase-specific quenching of fluorescent dyes. 1. nucleobase one-electron redox potentials and their correlation with static and dynamic quenching efficiencies. *J. Phys. Chem.*, **100**, 5541–5553.
32. Steenken,S. and Jovanovic,S.V. (1997) How easily oxidizable is DNA? One-electron reduction potentials of adenosine and guanosine radicals in aqueous solution *J. Am. Chem. Soc.*, **119**, 617–618.
33. Meisenheimer,K.M. and Koch,T.H. (1997) Photocross-linking of nucleic acids to associated proteins. *Crit. Rev. Biochem. Mol. Biol.*, **32**, 101–140.
34. Ito,T. and Rokita,S.E. (2003) Excess electron transfer from an internally conjugated aromatic amine to 5-bromo-2′-deoxyuridine in DNA. *J. Am. Chem. Soc.*, **125**, 11480–11481.
35. Hole,E.O., Nelson,W.H., Close,D.M. and Sagstuen,E. (1987) ESR and ENDOR study of the guanine cation: Secondary product in 5′-dGMP. *J. Chem. Phys.*, **86**, 5218–5219.